American Journal of Energy and Power Engineering
2017; 4(6): 89-97
http://www.aascit.org/journal/ajepe
ISSN: 2375-3897

AASCIT American Association for Science and Technology

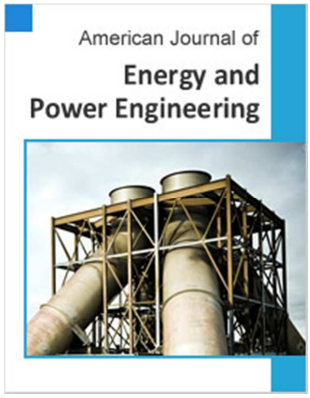

CFD Study of Flow Field Velocities and 3D Effects over the MEXICO Wind Turbine Model

Borja Plaza Gallardo[1], Rafael Bardera Mora[2], Sergio Visiedo Martínez[1]

[1]Ingenieria de Sistemas para la Defensa de España S. A. (ISDEFE), Madrid, Spain
[2]National Institute of Aerospace Technology (INTA), Madrid, Spain

Email address

bplaza@isdefe.es (B. P. Gallardo), barderar@inta.es (R. B. Mora), sergiovisiedo@gmail.com (S. V. Martínez)

Citation

Borja Plaza Gallardo, Rafael Bardera Mora, Sergio Visiedo Martínez. CFD Study of Flow Field Velocities and 3D Effects over the MEXICO Wind Turbine Model. *American Journal of Energy and Power Engineering.* Vol. 4, No. 6, 2017, pp. 89-97.

Abstract

The deep understanding about wake field and 3D effects of wind turbines are still a challenge, due to the complexity of the three-dimensional flow which blades rotation produces. In this work an aerodynamic analysis about wind turbine model MEXICO is realized, firstly of axial distribution of velocities in several regions inside the streamtube and then some estimations of 3D effects, either lift coefficient augmentation or stall delay phenomenon. CFD-RANS simulations have been carried out at three different wind speeds, and results are compared to experimental data of the MEXICO project, from wind tunnel tests. Results show that axial and radial inductions are greater for outer sections and lower as wind speed increases, providing different wake configurations. As for the 3D effects, it is found that rotational augmentation appears firstly for inner part of the blade and they advance progressively towards span-wise direction as wind velocity grows. For inner section, at high wind speed, lift coefficient increase reaches to values of 50% over the corresponding 2D polar curve.

Keywords

MEXICO,
Mexnext,
Aerodynamics,
CFD,
Axial Velocity,
Radial Velocity,
3D Effects

Received: September 27, 2017
Accepted: November 14, 2017
Published: December 6, 2017

1. Introduction

To study wind turbine aerodynamics it is important to know the effects than air yields to the rotor as well as the state of motion of the air along the streamtube, both upstream as downstream. Blade rotation produces velocity inductions to the air in all directions, generating the appearance of three-dimensional flows which makes the two-dimensional airfoil theory, used in many computational engineering codes, not valid to predict some phenomena. Important examples of these are 3D effects, which produce lift enhancement and stall delay in some airfoils of the blades, and its considerations is very important for an appropriate aerodynamic design. The intensity of the 3D effects depends on incoming wind speed and have a higher impact at inner section of the blades, as will be seen in discussion section.

In this work is analyzed the results, obtained by mean of RANS approach CFD simulations over the MEXICO experimental model, of axial traverse of two wind components (axial and radial velocities) to observe the influence of wind speed and the distance to the rotation axis in the wake configuration. Furthermore, an estimation of rotational augmentation produced by 3D effects is carried out to see the lift increase for three sections in the blade and the streamlines over the wall of the blade to see the separated flow regions.

The MEXICO experimental wind turbine is an instrumented horizontal axis three bladed machine, with 4.5 m rotor diameter. It was tested at the German-Dutch DNW wind tunnel in many different controlled conditions, where huge amounts of experimental data were taken. CFD simulations have been implemented in the commercial software Fluent 14.5 (ANSYS), using a HPC cluster to carry out the complex calculations with steady-RANS approach. In this article, some experimental data from MEXICO project [1] will be compared with calculations, which have been carried out at National Institute for Aerospace Technology of Spain (INTA), inside the Mexnext Project framework [2].

2. Methods

2.1. Mesh Generation

To generate the mesh, the software ICEM CFD 14.5 (Ansys) is used. An unstructured mesh has been computed instead of structured grid, since the number of elements is not high enough to look for saving computing time.

The MEXICO wind turbine 3D geometry has been designed in CATIA V5. The blades have the real geometry as defined in MEXICO Experimental Description [1] because they are the most important aerodynamic elements. Special attention has been paid to refine the grid over the blade surfaces.

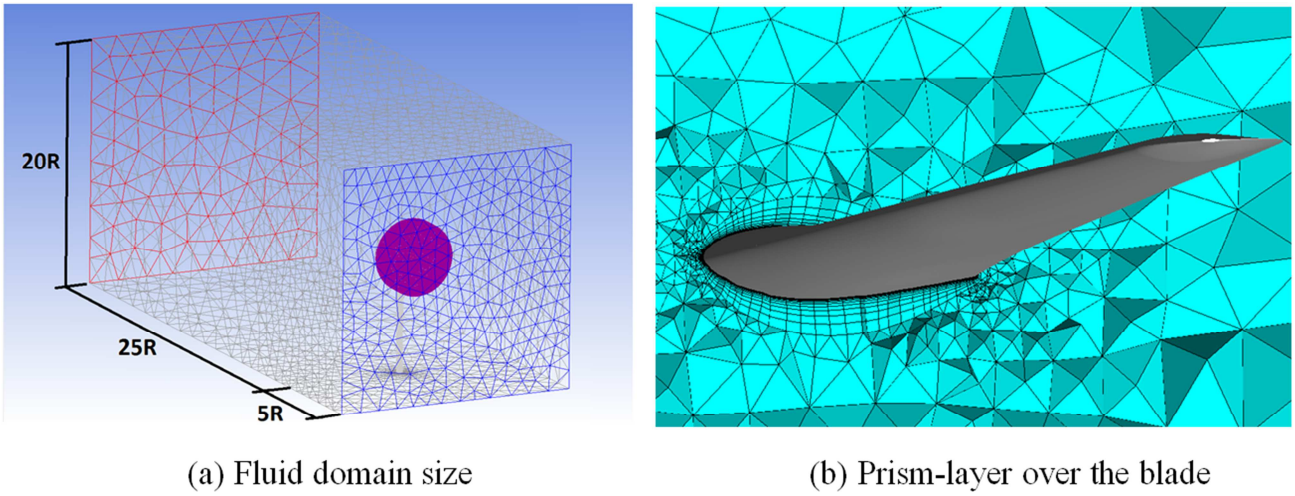

(a) Fluid domain size (b) Prism-layer over the blade

Figure 1. *Mesh details.*

Two different regions have been defined for fluid volume. A cylindrical domain of 2.75R diameter and 0.5R height contains the moving parts: blades and hub. A Moving Reference Frame is set to this region, applying to it the design wind turbine rotation speed of 4.5 rpm. The rest of the fluid domain inside the wind tunnel has an extension of 5R upwind from the rotor plane, 25R downwind and a width and height of 20R, as shown in Figure 1(a).

Boundary layer calculation is very important to obtain more accurate results in MEXICO rotor simulations. To capture correctly boundary layer phenomenon a prism layer is created covering all over the wind turbine surface. It is necessary to keep the factor $y^+<1$ after the computation because of the use of k-ω SST turbulence model for the simulations, so estimations for the nearest layer thickness give a value of 5×10^{-6} m. The successive layers grow progressively, as shown in Figure 1(b), up to a total of 20 layers.

The final result after the computation of the grid is an unstructured "tetra-prism layer" mesh of about 12 million elements. This is the appropriate number of elements to obtain a good compromise between accuracy in results and time calculation. However the mesh refinement has been focused in the rotor zone rather than the far field downwind from the rotor plane, as shown in Figure 2, and it will generate loss in precision of calculation at this region.

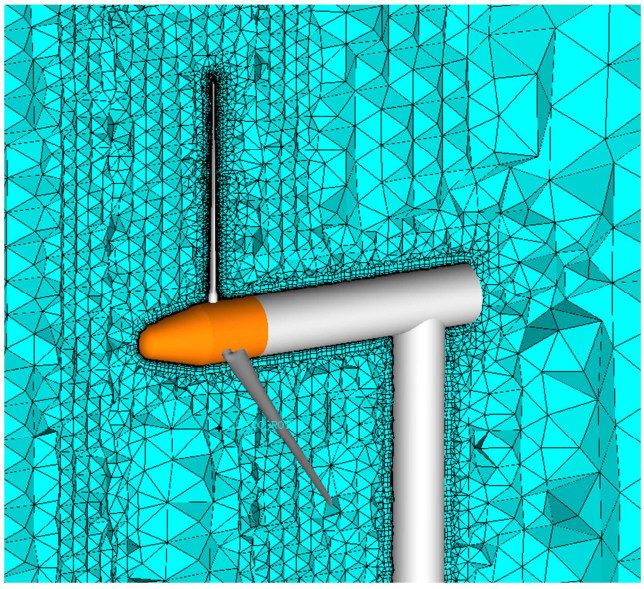

Figure 2. *"Tetra-prism layer" mesh.*

2.2. Features of Simulations

The computed CFD simulations implement a steady pressure-based model, with the Semi-Implicit Method for

Pressure-Linked Equation algorithm (SIMPLE) to solve Reynold's Averaged Navier-Stokes equations [3].

According to the available experimental data, simulations has been carried out for axial flow (no-yaw), pitch angle of -2.3° and a constant rotation speed of 424.5 rpm. Different cases with steady wind velocity between 5 m/s and 24 m/s has been computed, but results from only three cases are expose in this work. Those are representatives of turbulent wake state (U_∞=10 m/s, λ=10) design conditions (U_∞=15 m/s, λ=6.67) and separated flow conditions (U_∞=24 m/s, λ=4.17) and allow to observe how rotor loading affects to calculations.

As for the boundary conditions, they are set as "velocity inlet" (blue surface in Figure 1(a)) for the airflow entrance, "Pressure outlet" (red surface), "Symmetry" for the rest of the tunnel faces (grey) and "wall" for the surfaces of the wind turbine model. The cylindrical surface between the rotational and static domain is set as "interface" for a correct computation.

2.3. Flow Field Velocities

In the MEXICO wind tunnel experiments, axial (u), radial (v) and tangential (w) components of velocity were measured by mean of PIV technique [4] along two axial lines at the same rotation axis height and a distance from it of r=1.4m (~0.6R) and r=1.8m (0.8R), as shown in Figure 3, for each revolution when rotor azimuthal position was φ=0°. For CFD simulations, those three components are computed with the same configuration as experiment, but only axial and radial velocities will be studied. Thus are compared the differences between computed results and measurements in flow velocity disturbances, for both inner and outer sections, with blade 1 pointing to positive Z axis direction.

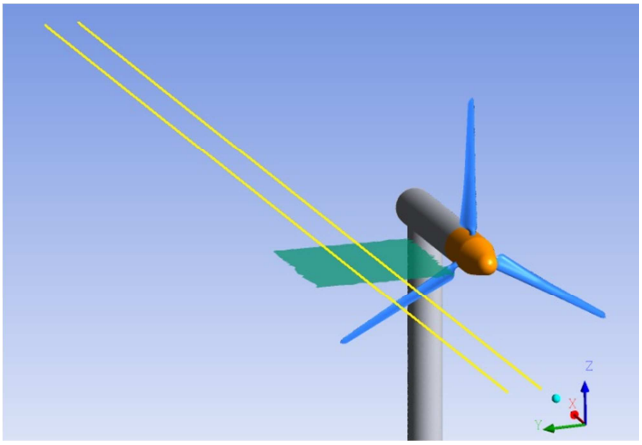

Figure 3. *Lines for axial traverse measurements of velocity.*

RANS approach simulations show results which are averaged values of the components of velocity for every location in the fluid domain, hence there are much lost information about unsteady effects as turbulent wake oscillations. However, it is possible to make a general analysis for the evolution of airflow, from the free stream at inlet to far downstream in the wake.

2.4. 3D Effects

The estimation of 3D effects is made comparing the results obtained in the described simulations with experimental two-dimensional polar curves (C_l-α_{2D}) provided in the ECN report [1] for Mexnext project at appropriate Reynolds numbers. To find different points for three-dimensional polar curves (C_l-α_{3D}), is calculated the lift coefficient C_l for the three different airfoils of the blade (25%, 60% and 95% spanwise section) and also the angle of attack is estimated.

It is known the difficulty for an accurate calculation of angle of attack for wind turbines blade from CFD calculations with 3D flow, and many different methods are proposed, either experimental, theoretical or computational ones [5, 6]. For this work a graphical method much simpler and faster than other, has been carried out, since the qualitative description does not require high precision in calculation. Hence the angle of attack is obtained directly from different images as Figure 9, measuring the angle between the chord of the airfoil and the farthest streamlines.

3. Results and Discussion

Following the described methodology in the previous section, results from RANS-CFD simulations are exposed: firstly, is made an analysis about the axial traverse for axial and radial velocity of the stream, and then a description and quantification of the 3D effects which affect to the blade aerodynamics and yield rotational augmentation.

3.1. Flow Field Velocities

As will be seen, the purely axial flow suffers a deceleration in stream-wise direction due to the pressure jump produced in the rotor plane, which defines the rotor loading and hence the downstream wake features. Blade rotation induces velocities to the flow, providing a tangential component (not discussed in this article) which generates a helical movement of the stream in the opposite direction of rotation, which moves downstream along the wake. The pressure jump through the rotor plane also produces a radial velocity induction which results in the streamtube expansion, although this induction is also related with vortex shedding in hub and blade tip region [7]. Next paragraph, the axial and radial components of flow velocity are exposed, both results and MEXICO experimental data, for the three different wind speed or in other words, tip speed ratios (λ), comparing them each other.

Axial Velocity

Figure 4 shows the curves of non-dimensionalised axial velocity by the corresponding freestream velocity ($\tilde{u} = u/U_\infty$), plotted in function of non-dimensionalised axial coordinate ($\tilde{x} = x/D$). The relative descends in axial velocity are observed at both inner and outer sections for different wind speed.

At first sight the deficit between measurements and calculations of velocity upwind before the stream crosses the

rotor, highlights. This difference is lower as the velocity of incoming wind is higher, and the highest velocity case (λ=4.17), calculations are in good agreement with experimental data. This consequence of a weak convergence of the code and also an incorrect prediction of velocity distribution in the wake, resulting in that poor estimation upstream.

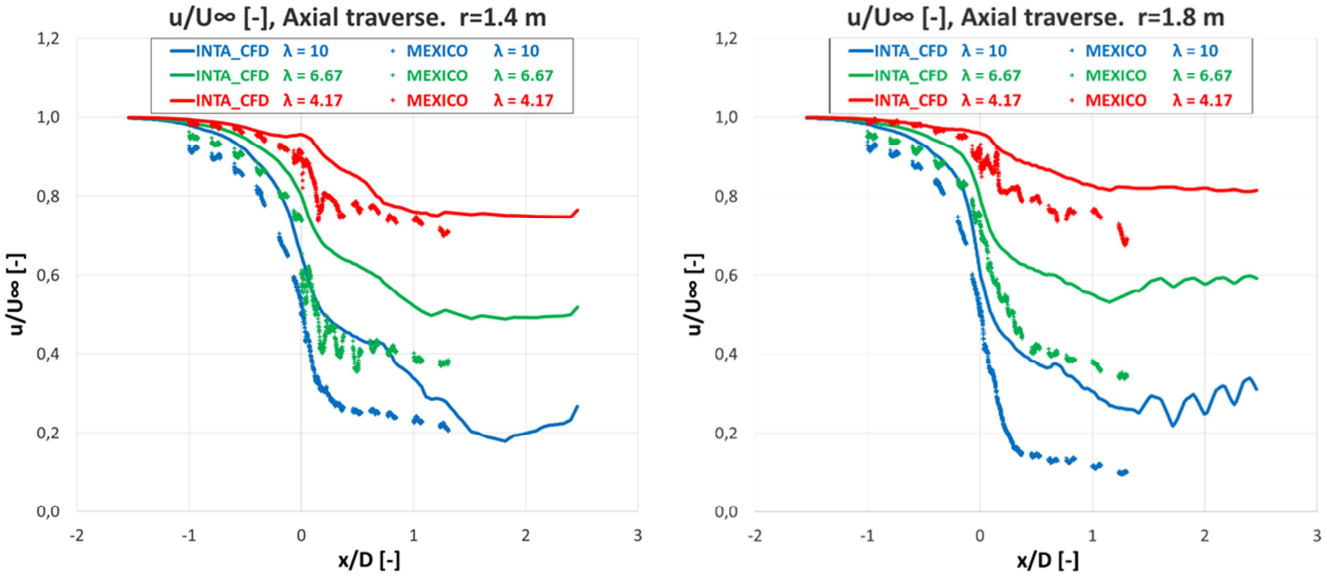

Figure 4. *Axial traverse of non-dimensional axial velocity.*

As tip speed ratio value grows, so do the decrease of relative velocity downstream in the wake. Hence the rotor loading and axial induction are higher for lower wind speeds. Looking at two graphs can be seen that, for outer sections, experimental data show lower axial velocities in the wake (in other words, more induction) as expected. However, CFD results predict a lighter induction for inner sections. A possible explanation is that vortex shedding at tip region produces more induction at outer sections, and it cannot be predicted by the RANS simulations implemented, due to the thickness of the mesh and the overly dissipative nature of the used turbulence models.

For design conditions (λ=6.67), is noticeable a high descend in axial velocity, as expected, but not such high as experimental data show, since it should be about 40% of freestream velocity, for outer section and at a distance of 1 diameter downstream. This is well predicted in [10] and [11], but in this work results give values of 55%. In the last reference, some different CFD codes used for Mexnext project demonstrates that an Unsteady-RANS simulation can improve the predictions, although a general overestimation is still view.

With a tip speed ratio λ=10, the rotor is working at turbulent wake state and the computed parameter $\tilde{u}$ reach to values of 0.2 for inner section, as the experimental measurements, but it is delayed half a diameter. For outer section and the same wind speed, differences between experimental and computed results become in the order of 20%. These discrepancies are reduced to 10% in the highest incoming wind velocity case (λ=4.17).

For the three computed cases there is a high overestimation in the nearest wake to the rotor plane. LES and DES simulations [8, 9] could improve the results in estimating axial velocities because of the much better predictions of turbulence phenomena and dissipation in the near wake region.

Radial Velocity

Curves of non-dimensional radial velocity ($\tilde{v} = v/U_\infty$) are represented as function of non-dimensional axial coordinate ($\tilde{x} = x/D$) in Figure 5. For inner and outer sections can be seen the induction of velocity in radial direction, which show a peak very close to the rotor plane ($\tilde{x} = 0$). This gives an idea of the wake expansion, because of it is a positive velocity towards span-wise direction. The quick decrease after this peak reflects the loss of radial component in airflow and hence the progressive change of direction of streamlines which become fundamentally axials.

As for the experimental data measured in wind tunnel, must be mentioned the high spread due to the difficulty for measurements of radial velocities (relatively small) by mean of PIV techniques for a three-dimensional flow, which presents oscillations as consequence of blade rotation. Nevertheless, the trend and magnitude of these velocities can be observed.

According to results, the radial velocity increasing for inner section is between 5% and 10% of wind speed, while for outer section is from 10% to 25%, what shows that the streamlines open further for the outer station.

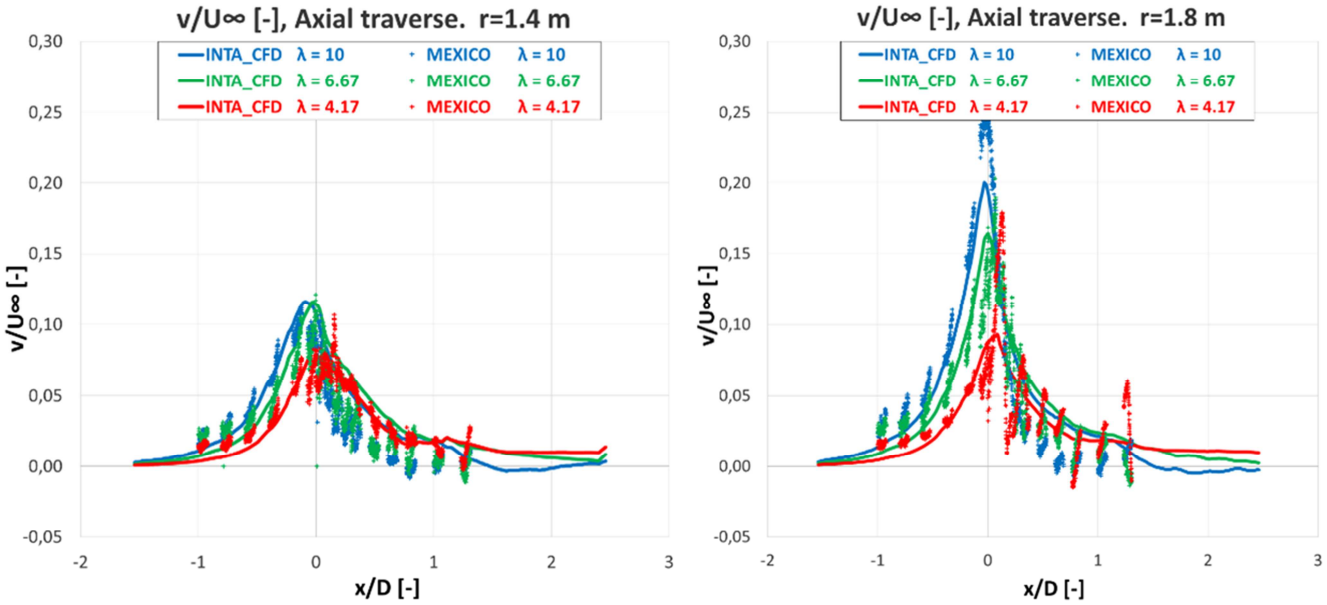

Figure 5. *Axial traverse of non-dimensional radial velocity.*

Looking at Figure 5 can be observed a good approximation of simulation results to MEXICO experimental measurements for inner section at all three wind speeds. However, results for outer section are slightly underestimated at peaks, especially when U_∞=24 m/s. At this wind speed, experimental data show a pronounced peak of unknown causes, and there are some doubts about measurements. It is possible that the outer region of the blade is influenced by tip vortex, which cannot be predicted accurately by CFD code.

As happened to axial velocity an overestimation of radial component is observed in near wake region for high values of λ parameter. However, at low rotor loading (λ=4.17), calculations show good results in spite of the no prediction of oscillations at $r = 1.8\,m$ in the wake observed in experimental data.

Hence in Figure 5 is seen that radial induction is higher for outer section of the blade, implying more pronounced deviations of the stream than inner stations.

This induction increases as wind speed is lower, resulting in higher wake expansion which generate the different wakes shapes of Figure 6. Looking at these three images can be see the contours of the non-dimensional stream velocity $\left(\tilde{V} = V/U_\infty\right)$, and it is observed this wake expansions for each wind velocity case. As shown, the width of wake is higher at greater rotor loading, i.e. at lower incoming flow velocity. The red zone shows the freestream velocity in each case ($\tilde{v} = 1$) and a higher colors contrast represents more differences in velocity magnitude. Hence, can be deduced that for λ=10 exist a re-energization process of wake slower than λ=4.17 case, because the further deceleration of stream causes lower diffusion in vorticity behind the rotor plane. This is also the reason to explain that the length of lowest speed region in the wake is higher for lower wind speed, resulting in a longer wake.

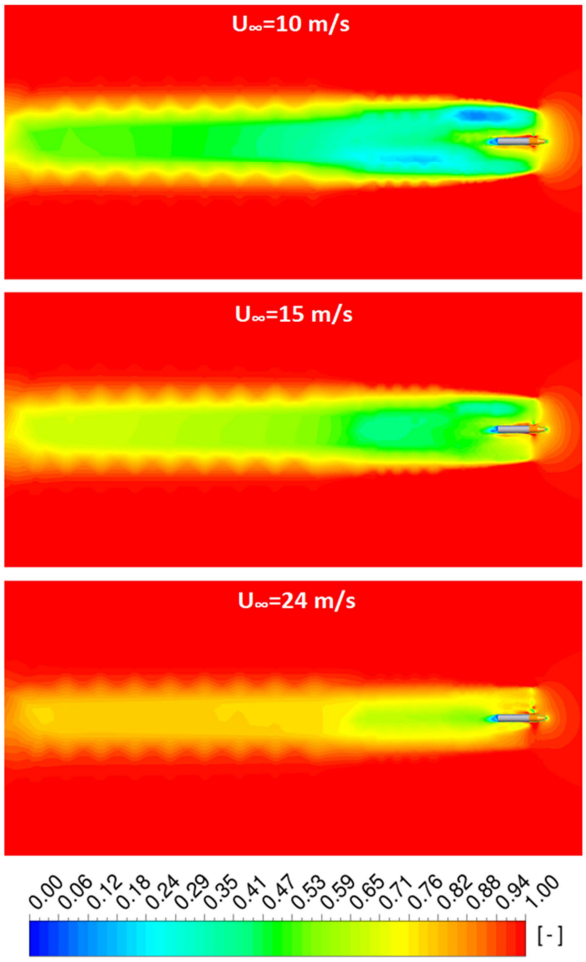

Figure 6. *Different wake configurations at different wind speed. Colors show the non-dimensional velocity magnitude.*

3.2. 3D Effects

To study 3D effects, C_l- α_{2D} and C_l- α_{3D} polar curves for

the three airfoils of the blade are plotted as explained in Section 2.4. Despite the values of angles of attack for 3D polar are estimations (3 points per each airfoil), graph in Figure 7 show the effect of rotational augmentation. For section 25% (DU91—W2-250 airfoil), is noticeable the lift coefficient increase as consequence of 3D effects which blade rotation produces.

In the other hand, for 95% station (NACA 64-418 airfoil), the estimation of C_l- α_{3D} curve from CFD results is under the corresponding two-dimensional experimental polar curve of the airfoil. This is expected because of the tip loss, which reduces drastically the lift force in this region of the blade. At 60% section of the blade (RISØ-A1-21 airfoil), results also show a slightly increment of lift coefficient and the stall delay is perceptible as shows the last green circle (the higher estimated angle of attack for this station, at highest wind speed 24 m/s).

More accurate results about rotational augmentation can be seen in [12], but the estimations for the present work show, as expected, that 3D effects have much more influence at the inner part of the blade, where the lift coefficient increase for 3D curves with respect to 2D's, reaches to values of 50%.

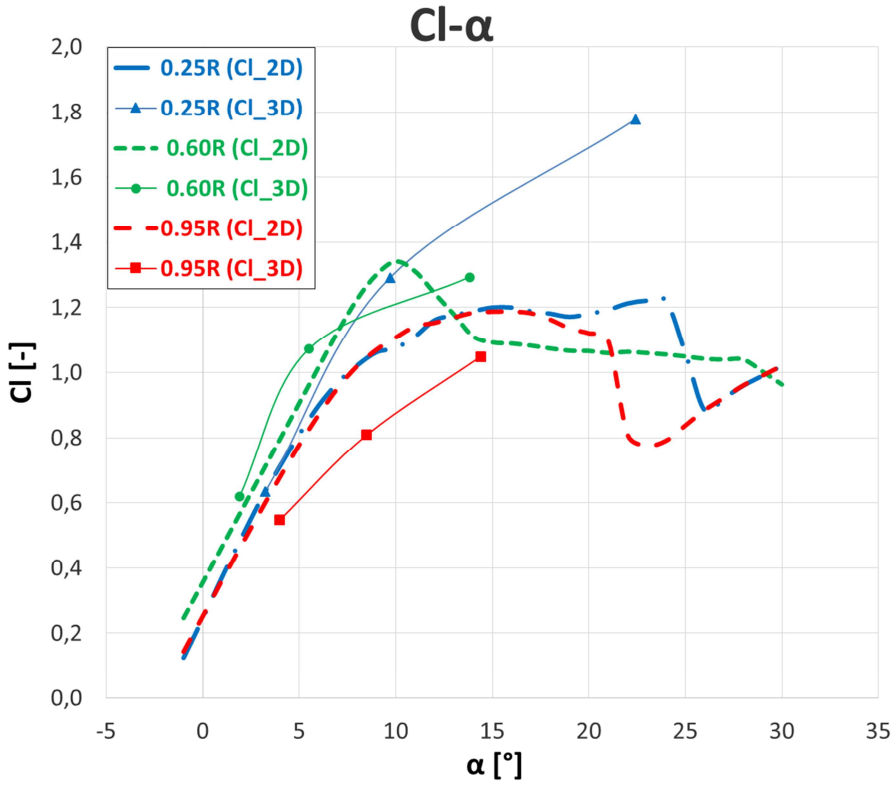

Figure 7. *Polar curves for three sections of the MEXICO blade.* C_l- α_{3D} *vs.* C_l- α_{2D}.

The origin of the physical phenomenon to explain the stall delay is still under discussion. When an airfoil is rotating, the stall may occur at higher angles of attack than the equivalent 2D curve from static wind tunnel test at the same Reynolds number. It is known that adverse gradients of pressure suffered by airflow over the suction side of the blade, produce a slowdown in the flow near the trailing edge, as in the boundary layer. The combination of both may become to zero the flow velocity in that region, or even a reverse flow. If this inversion of flow direction happens, the separation occurs and the airfoil is in stall conditions. That adverse pressure gradient is reduced for unknown reasons by blade rotation but the next explanation is accepted: this rotation produce an increase of dynamic pressure in span-wise direction which, besides the centrifugal force experienced by air particles, result in a radial induction to the flow. This radial component of velocity generates the appearance of Coriolis force which redirect the flow towards the trailing edge. The Coriolis force induces a positive pressure gradient which causes re-attachment to the flow and delays the separation [13, 14].

Looking at streamlines over the suction side of the blade at different wind speeds, can be understood what happens to the near wall flow. When fluid particles start to experience the radial component of velocity the rotational augmentation begins. In Figure 8 can be seen these streamlines (oil flow) at 10, 15 and 24 m/s, where vortex regions and reverse flow (which determines the flow separation as deduced by *Guntur et al.* [15] and *Mukesh* [16]) are seen. At wind speed of 10 m/s the flow is attached to the whole of the blade, as shown in Figure 8 (a); however, at inner region near the hub, can be seen a radial component which is probably consequence of vortex shedding in this zone [17].

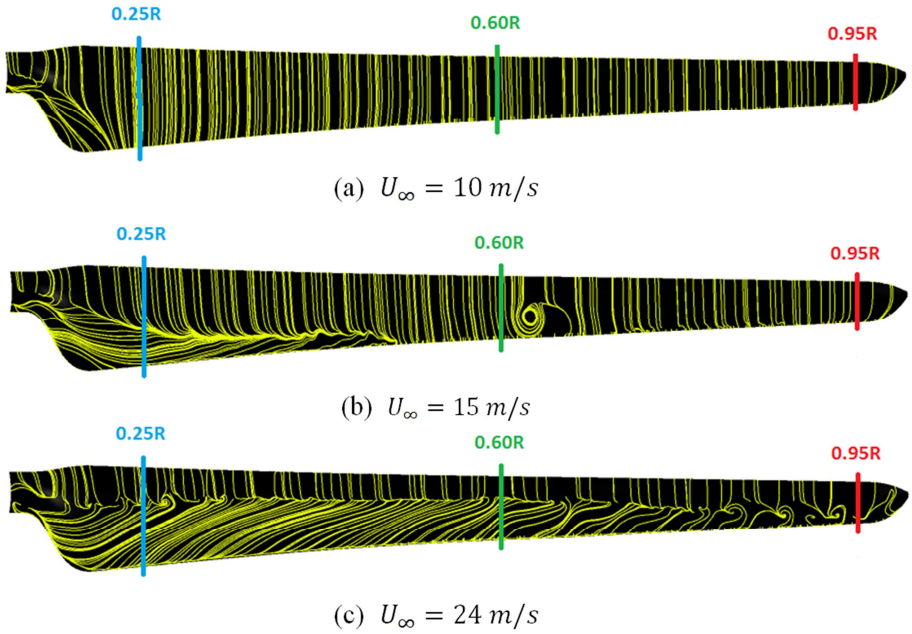

Figure 8. *Suction side streamlines on MEXICO blade at different wind speed.*

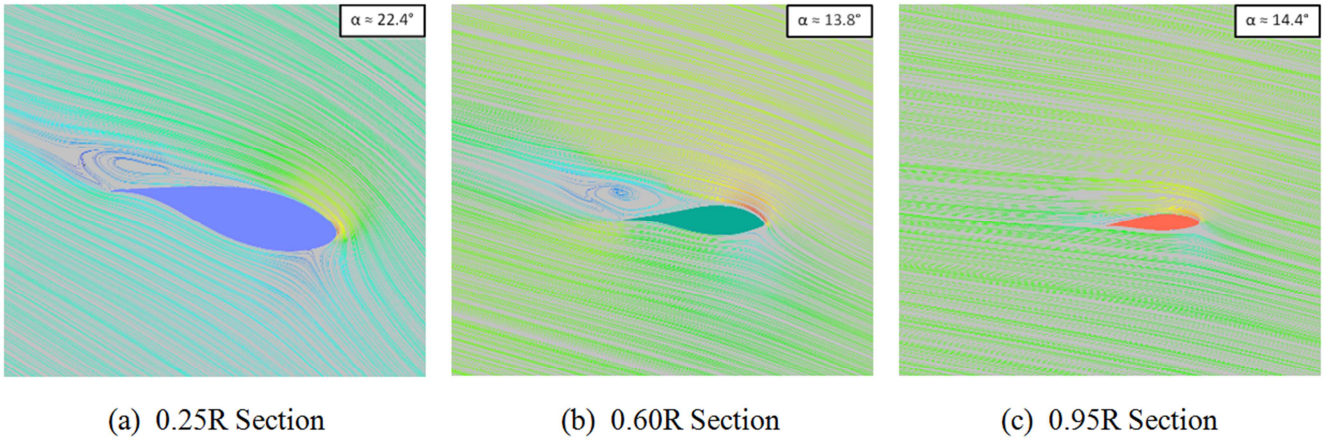

Figure 9. *Streamlines around the three studied sections and estimated angle of attack at 24 m/s wind speed.*

When U_∞=15 m/s it is observed a strong radial component near the trailing edge of the blade which covers the length from the hub to 45% of radius, where flow starts to be reverse and hence detached. It can be seen the line of flow separation which is the confluence of reverse streamlines. At first sight to Figure 8(b) one could think that 25% section is in stall conditions; however the direction of streamlines are not towards leading edge (the chord wise velocity does not less than zero) and, as seen in Figure 10(a), the flow is attached to the airfoil.

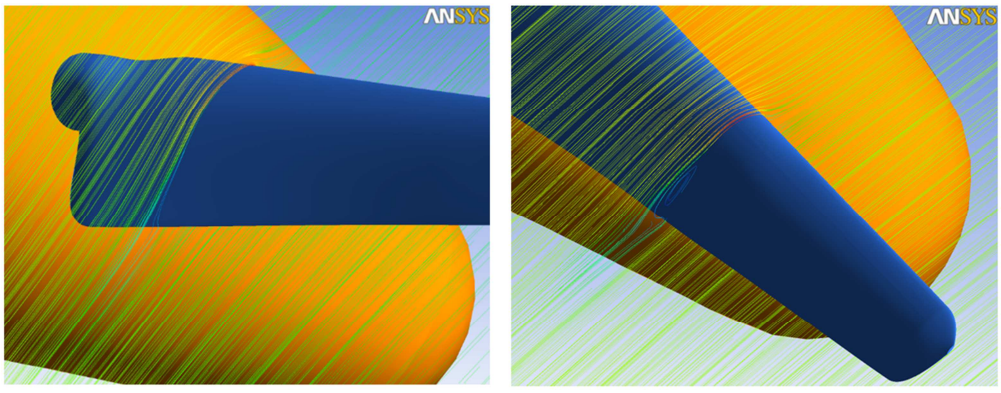

Figure 10. *Streamlines over two airfoils at 15 m/s wind speed.*

It is interesting to observe in Figure 8(b) the mid-span vortex near the 60% section. The cause of its appearance is unknown, although may be due to any phenomenon inducted by the abrupt transition between airfoils RISØ-A1-21 y NACA 64-418, very close to this section. In Figure 10(b) can be seen the detached flow produced by this vortex.

For the case at wind speed of 24 m/s (Figure 8(c)) can be seen that particles have reverse direction, from trailing edge towards leading edge, in suction side for the whole blade, which causes separation of boundary layer from about 30% chord-wise. Hence, almost all the blade in under stalled conditions. Is important to note, as seen previously.

4. Conclusions and Future Works

The aim of this work is to realize a descriptive analysis about the effects caused by three-dimensional flow over the MEXICO rotor and vice versa. A study about velocity field has been carried out by mean of axial traverse for axial and radial components, comparing the results obtained in RANS-CFD simulations with experimental data from MEXICO wind tunnel tests. In addition, a quantification of 3D effects which affects to blades aerodynamics is discussed.

For axial component of velocity it is observed a pronounced overestimation behind the rotor, higher as wind speed decrease, because the turbulent wake makes the calculation difficult with this kind of steady simulation. Capturing some non-stationary phenomena and making mesh refinements in wake region could improve the accuracy of results, so URANS simulations could be more appropriate. Differences in two studied stations show that outboard section provides higher induction of axial velocity than the inboard one, as expected.

The radial component shows that, as evident, the streamtube expands when the airflow crosses the rotor plane. Fluid particles experience a strong radial acceleration as they approach to the rotor, reaching the maximum of radial velocity very close to rotor plane and decaying behind it. These peaks have better predictions for inner sections, since the vortex shedding at tip region affects to the computation and even the experimental measurements at outboard region. It is also deduced than wake expansion is higher for lower wind speeds, as seen in the magnitude of peaks.

As for the 3D effects, the analysis shows that the lift augmentation affects widely to inner sections and decrease radially towards the blade tip, and the intensity of them is higher as higher wind speed, due to the higher gradients of pressure along the blade. Moreover, the stall delay appears at the highest wind speed condition as seen for 60% blade section, whose 3D lift coefficient C_l is over the 2D polar curve at stall region.

Future investigations should implement simulations DES or LES for a complete wind turbine model, to make more suitable studies about diffusion at wake region, vortex calculations and instability phenomena which cannot predict the more current techniques. A deep study about velocity distribution in the wake and 3D effects could help to develop new models and methods to improve both accuracy and time of computation.

References

[1] K. Boorsma and J. G. Schepers, *Description of experimental setup MEXICO measurements*, ECN-X-11-120, Energy research Centre of the Netherlands (ECN), March 2009.

[2] J. G. Schepers, K. Boorsma, T. Chon, Niels Sørensen, *Final report of IEA Task 29, Mexnext (Phase 1): Analysis of Mexico wind tunnel measurements*, ECN-E-12-004, Energy research Centre of the Netherlands (ECN), February 2012.

[3] Jasak H, *Error analysis and estimation for the finite volume method with applications to fluid flows*, PhD thesis, Imperial College of Science, Technology and Medicine, 1996.

[4] Raffel, M., Willert, C. E., Wereley, S. T. & Kompenhans, J., "Particle Image Velocimetry" –A Practical Guide-, Second Edition, Springer-Verlag Berlin, 2007.

[5] Srinivas Guntur and Nierls N. Sørensen, *An evaluation of several methods of determining the local angle of attack on wind turbine blades*, Proceedings of Science of Making Torque from Wind, Oldenburg, Germany, October 2012.

[6] Horia Dumitrescu, Vladimir Cardos, Florin Frunzulica, Alexandru Dumitrache, *Determination of angle of attack for rotating blades,* POLITEHNICA University of Bucharest, Bucharest, Romania, 2012.

[7] Daniel Micallef, Gerard van Bussel, Carlos Simao Ferreira, and Tonio Sant, *An investigation of radial velocities for a horizontal axis wind turbine in axial and yawed flows*, Wiley Online Library, 2012.

[8] Yuwei Li, Kwang-Jun Paik, Tao Xing, and Pablo M. Carrica, *Dynamic overset CFD simulations of wind turbine aerodynamics*, Renewable Energy 37: 285-298, 2012.

[9] J. Johansen, N. N. Sørensen, and J. A Michelsen ans S. Schreck, *Detached-eddy simulation of flow around the NREL Phase VI blade*, Volume 5, Issue 2-3, pages 185–197 April-September 2002, July 2002.

[10] H Snel, J G Schepers, and B Montgomerie, *The MEXICO project (Model Experiments in Controlled Conditions): The database and first results of data processing and interpretation*, The Science of Making Torque from Wind, Journal of Physics: Conference Series 75, IOP Publishing, 2007.

[11] J. G. Schepers, K. Boorsma, T. Cho, S. Gomez-Iradi, P. Schaffarczyk, A. Jeromin, W. Z. Shen et al., *Review of computational fluid dynamics for wind turbine wake aerodynamics*, Energy research Centre of the Netherlands (ECN), February 2012.

[12] J. G. Schepers, K. Boorsma, H. Snel, *IEA Task 29 Mexnext: Analysis of wind tunnel measurements from the EU project Mexico*, The Science of Making Torque from Wind.

[13] Hsiao Mun Lee and Leok Poh Chua, *Investigation of the stall delay of a 5kW horizontal axis wind turbine using numerical method*, International Conference on Renewable Energies and Power Quality (ICREPQ 12), Santiago de Compostela, Spain, March 2012.

[14] Tony Burton, Nick Jenkins, David Sharpe, and Ervin Bossanyi, *Wind Energy Handbook*, John Wiley & Sons, Ltd. ISBN: 978-0-470-69975-1, West Sussex, PO19 8SQ, United Kingdom, 2011.

[15] Srinivas Guntur and Niels N. Sørensen, *A study on rotational augmentation using CFD analysis of flow in the inboard region of the MEXICO rotor blades*, Wiley Online Library, January 2014.

[16] Mukesh M. Yelmule and EswaraRao Anjuri VSJ, *CFD predictions of NREL Phase VI Rotor Experiments in NASA/AMESWind tunnel*, INTERNATIONAL JOURNAL of RENEWABLE ENERGY RESEARCH, June 2013.

[17] Akay B, Ragni D, Simo Ferreira C, and van Bussel G, *Experimental investigation of the root flow in a horizontal axis wind turbine*, Wind Energy. DOI: 10.1002/we.1620, 2013.